Improved dynamic geomagnetic rigidity cutoff modeling: testing predictive accuracy

Mark A. Clilverd

Physical Sciences Division, British Antarctic Survey (NERC), Cambridge, United Kingdom

Craig J. Rodger

Department of Physics, University of Otago, Dunedin, New Zealand

Tracy Moffat-Griffin

Physical Sciences Division, British Antarctic Survey (NERC), Cambridge, United Kingdom

Pekka T. Verronen

Finnish Meteorological Institute, Helsinki, Finland.

Abstract. In the polar atmosphere, significant chemical and ionization changes occur during solar proton events (SPE). The access of solar protons to this region is limited by the dynamically changing geomagnetic field. In this study we have used riometer absorption observations to investigate the accuracy of a model to predict K_p-dependent geomagnetic rigidity cutoffs, and hence the changing proton fluxes. The imaging riometer at Halley, Antarctica is ideally situated for such a study, as the rigidity cutoff sweeps back and forth across the instrument's field of view, providing a severe test of the rigidity cutoff model. Using observations from this riometer during five solar proton events, we have confirmed the basic accuracy of this rigidity model. However, we find that the model can be improved by setting a lower K_p limit (i.e., K_p=5 instead of 6) at which the rigidity modeling saturates. We also find that for L>4.5 the apparent L-shell of the beam moves equatorwards. In addition, the Sodankyla Ion and Neutral Chemistry model is used to determine an empirical relationship between integral

proton precipitation fluxes and nighttime ionosphere riometer absorption, in order to allow consideration of winter time SPEs. We find that during the nighttime the proton flux energy threshold is lowered to include protons with energies of >5 MeV in comparison with >10 MeV for the daytime empirical relationships. In addition, we provide an indication of the southern and northern geographic regions inside which SPEs play a role in modifying the neutral chemistry of the stratosphere and mesosphere.

1. Introduction

Solar proton events (SPEs) are a major space weather phenomena that can produce hazardous effects in the near-Earth space environment. The occurrence of SPEs varies during the 11-year solar activity cycle. In active years, especially during the falling and rising phases of the solar cycle, SPEs may average one per month, but during solar minimum years the occurrence is very low, e.g., ~1 per year. SPEs cause 'upsets' to Earth-orbiting satellites, increased radiation exposure levels for humans onboard spacecraft and high-altitude aircraft, ozone depletions and disruption to HF/VHF communications in mid- and high-latitude regions. A detailed understanding of all these impacts depends upon knowledge of the dynamic rigidity cutoffs as SPE particles are partially guided by the geomagnetic field. Higher rigidities are required for a particle to reach lower geomagnetic latitudes, and thus all particles with rigidities larger than the minimum can penetrate to that latitude (and all higher latitudes). The geomagnetic cutoff rigidity is a dynamic quantity depending on the Earth's internal and external magnetic fields [*Smart and Shea*, 2003; *Kress et al.*, 2004].

Experimental measurements of geomagnetic cutoff rigidities have generally been based on satellite observations. Few experimental studies have derived cutoffs during the most disturbed conditions during geomagnetic storms. Theoretical calculations have primarily focused on tracing particles through models of the Earth's field producing grids of estimated cutoff rigidities distributed over the Earth at a given altitude [e.g., *Smart and Shea*, 2001]. *Birch et al.* [2005] used satellite measurements of the edge of the polar cap sampled four times each day, and found that cutoff latitudes reduce by 5-8º during storms. They compared the results with particle-tracing models, which underestimated the effects of a severe storm. *Rodger et al.* [2006] used the model of K_p-dependent geomagnetic rigidity cutoff energies based on the Tysganenko-89 magnetic field model [*Smart and Shea*, 2001], to investigate for the first time, detailed comparisons of theoretical cutoff rigidities and ground-based measurements during a large

54 geomagnetic disturbance. Energy cutoffs on satellite derived proton fluxes were used to calculate
55 the predicted cosmic noise absorption levels for the Halley imaging riometer (IRIS) during a
56 single SPE event in November 2001. The predicted absorption levels showed good agreement
57 with those experimentally observed for low and mid levels of geomagnetic disturbance levels
58 (K_p<5). However, in very disturbed conditions (K_p≈7-9) the rigidity energy cutoffs indicated by
59 the IRIS observations appeared to saturate around those predicted for K_p≈6 by the particle-
60 tracing approach. This suggested that the geomagnetic latitude limit for the penetration of SPE
61 protons during large geomagnetic storms is rather more poleward than had been indicated
62 previously.

63 Imaging riometer systems (IRIS) like the one at Halley, Antarctica, are well suited for
64 examining geomagnetic cutoffs, because the receiver arrays provide an image of the ionospheric
65 absorption levels in a 200 km × 200 km horizontal region above the instrument by measuring the
66 absorption of cosmic radio noise at a given frequency (usually 20-40 MHz). Using riometers it
67 has previously been shown that there is an empirical relationship between the square root of the
68 integral proton flux (>10 MeV) and cosmic noise absorption (CNA) in daytime, at least when
69 geomagnetic cutoff effects do not limit the fluxes [*Kavanagh et al.*, 2004]. The same study
70 concluded that variations in the spectral hardness of the SPE proton flux and atmospheric
71 collision frequencies do not cause significant departures from the linear relationship observed.

72 In this paper we examine ground-based measurements during five SPEs, based on the
73 observations from the imaging riometer at Halley, Antarctica, which is situated such that the
74 rigidity cutoff sweeps back and forth across the instrument's field of view during each SPE. We
75 calculate riometer absorption, using input proton fluxes modified by rigidity cutoff calculations,
76 and contrast the varying, predicted and observed, rigidity cutoffs during each geomagnetic
77 disturbance. We also use the Sodankyla Ion and Neutral Chemistry (SIC) model to determine an
78 empirical relationship between integral proton precipitation fluxes and nighttime ionosphere

riometer absorption to complement the daytime relationship already published, and to study rigidity effects during winter time SPEs.

2. Experimental Setup

The riometer utilizes the absorption of cosmic radio noise by the ionosphere [*Little and Leinbach*, 1959] to measure the enhancement of D-region electron concentration by energetic charged particle precipitation [*Stauning*, 1996]. The riometer technique compares the strength of the cosmic radio noise signal received on the ground to the normal sidereal variation referred to as the quiet-day curve to produce the cosmic noise absorption. The instantaneous ionospheric absorption in decibels is derived from the ratio of the prevailing signal level to this curve [*Krishnaswamy et al*., 1985]. In typical operations the absorption peaks near 90 km altitude, where the product of electron density and neutral collision frequency maximizes. In this paper we consider experimental observations from selected beams of an imaging riometer located at Halley (75.6ºS, 26.32°W, L=4.6), as shown in Figure 1.

At Halley the system is a snow-buried 49-beam imaging riometer, operating at 38.2 MHz and sampled every 1 sec [*Rose et al.*, 2000]. Several receivers are multiplexed through a phased array of 64 crossed-dipole antennas to achieve narrow beam scanning of the D region. The beam width is 13º. In the meridian plane the most equatorward and poleward beams intersect the D region ionosphere about 1º north (equatorward) and south (poleward) from the vertical central beam, respectively. Absorption values for obliquely orientated (non-vertical) beams are automatically corrected to vertical following the technique described by *Hargreaves and Jarvis* [1986].

In this study we analyze data collected at Halley during five SPEs. The SPE periods are July 2000, November 2000, two periods in November 2001, and October 2003. Prior to, and after these events the Halley imaging riometer performance was severely limited by snow buildup as

the IRIS was buried [*Rose et al.*, 2000] as a result of ever-increasing snow accumulation on the antenna array.

3. Estimates of Rigidity Cutoffs

It has been recognized for some time that geomagnetic rigidity cutoffs are well-ordered in terms of the McIlwain *L*-parameter [*Smart and Shea*, 1994; *Selesnick et al.*, 1995]. The *L*-variation of the geomagnetic rigidity cutoff has been determined for quiet times from ≈10,000 nuclei observations made by the MAST instrument on the SAMPEX satellite [*Ogliore et al.*, 2001]. These authors report that the geomagnetic rigidity cutoffs, R_c, for quiet times are given by

$$R_c = 15.062\ L^{-2} - 0.363 \qquad \text{(in GV)} \qquad (1)$$

representing average conditions for K_p=2.3. As noted above, dynamic vertical cutoff rigidities dependent upon magnetic activity levels have been determined by particle-tracing [*Smart and Shea*, 2003] using the K_p-dependent Tsyganenko magnetospheric field model. These authors have reported that the change of proton cutoff energy with K_p is relatively uniform over the range of the original *Tsyganenko* (1989) model (K_p<5), but the cutoff changes introduced by the *Boberg et al.* [1995] extension to higher K_p is non-linear such that there are large changes in proton cutoff energy for a given *L*-value at large K_p values. *Rodger et al.* [2006] made use of the K_p-dependent variations in the effective vertical cutoff energies at a given IGRF *L*-value at 450 km altitude determined from this modeling [*Smart et al.*, Fig. 5, 2003], but with a slight modification to ensure that the geomagnetic rigidity cutoff varies as 15.062 L^{-2}, as observed in the SAMPEX experimental data. Note that the change in cutoff energy with geomagnetic activity is strongly non-linear at the highest disturbance levels. In order to interpolate down to lower altitudes (e.g., 100 km), *Rodger et al.* [2006] followed the approach outlined by *Smart and Shea* [2003] again using the IGRF determined *L*-value. This exploits the basic relationship between R_c and *L*, i.e.,

$$R_c = V_k L^{-2} \quad (2)$$

where V_k is an altitude independent constant. Thus by knowing the value of V_k for the IGRF L-value at 450 km altitude above a given location, one can determine R_c at 100 km once one knows the L-value for that location at 100 km altitude. In the Rodger-approach the upper limit for K_p in the rigidity model is K_p=6. When K_p exceeds this level then it is forced to K_p=6 in the rigidity calculations, a limit selected through contrast with the November 2001 experimental observations.

The rigidity cutoff relationship developed by *Smart and Shea* [2003], and tested and improved by *Rodger et al.* [2006] is further investigated here using a series of SPEs observed by the imaging riometer at Halley.

4. Daytime riometer data and calculated absorption

Figure 2 shows three days of experimentally-observed cosmic noise absorptions recorded by two of the meridional beams of the Halley IRIS instrument (i.e., pointing N-S) during the 8-11 November 2000 SPE with 15 min averaging. In the upper panel CNA are shown for the IRIS southernmost beam 1 (L=4.80, solid line, which we term the "poleward beam"), and in the middle panel the northernmost beam 7, (L=4.32, long dashed line, which we term the "equatorward beam"). The beams map to the ionosphere so as to be viewing ~1º north and south in latitude (i.e. 75.6ºS ±1º). These two beams represent the two most extreme locations for rigidity cutoff effects that the instrument can observe. The bottom panel shows the variation of K_p during the SPE. In addition, both the upper and middle panels show the variation of the non-cutoff absorption that would be expected if there were no influence of rigidity on the proton fluxes into the atmosphere (short dashed line) based on the relationship between daytime absorption and proton fluxes developed by *Kavanagh et al.* [2004], i.e., using Absorption=0.09 × (>10 MeV proton flux)$^{0.5}$. This line therefore represents the variation of the proton fluxes

152 throughout the event. The equivalent absorption levels using rigidity affected proton fluxes
153 determined through the approach outlined in section 3 for each beam location are also shown
154 (asterisk in the south, diamond in the north), again calculated using the *Kavanagh et al.* [2004]
155 relationship. The time resolution of these calculations is limited to 3-hours because of the K_p
156 dependence of the rigidity cutoff model.

157 The SPE of 8-11 November 2000 generated peak GOES proton fluxes of 14,800 >10 MeV
158 protons cm^{-2} str^{-1} s^{-1} at 16 UT on 9 Nov, and a peak K_p of 6^+ at 9-12 UT on 10 Nov. As such, this
159 event occurred during a moderate geomagnetic storm. During November the atmosphere above
160 Halley, Antarctica, is fully sunlit and thus the use of the *Kavanagh et al.* [2004] daytime
161 absorption relationship is appropriate. In the southern (poleward) beam absorption levels of
162 ~4 dB are observed during the period of highest proton fluxes, while in the northern
163 (equatorward) beam absorption levels of ~2 dB are observed. These values are generally in good
164 agreement with the estimated absorption levels when the effects of varying rigidity cutoffs are
165 included, and significantly below the non-cutoff levels of ~8 dB absorption. When the proton
166 fluxes are very low the predicted absorption remains close to zero whatever the K_p level, thus it
167 is only possible to compare the predicted absorption with the observed absorption when the
168 proton fluxes are elevated. For the SPE of 8-11 November 2000 this is after 00 UT on 9 Nov,
169 lasting until the end of 10 Nov. Of the fifteen 3-hourly bins, 5 show significant over estimates
170 (~2 dB) in the predicted absorption in the southern (poleward) beam, while only 2 over estimates
171 occur in the northern (equatorward) beam. The remaining periods show reasonable agreement
172 between the predicted and observed absorption levels typically to within ±0.5 dB. Periods where
173 the absorption is higher than the predicted absorption level are likely to be influenced by
174 additional factors such as electron precipitation [*Shirochkov et al.*, 2004], which leads to
175 additional absorption on top of the proton-induced absorption, and are therefore not well
176 described by the proton-only *Kavanagh et al.* [2004] relationship. One example of this

occurrence is 00-06 UT on 9 November 2000, where higher than predicted absorption is seen on both beams.

There are two periods where the data and theory disagree during the 8-11 November 2000 event. At 6-12 UT on 10 Nov K_p reaches 6, and the theoretical absorption levels are the same as the non-cutoff case, i.e., a very high proportion of the proton fluxes should be impacting the atmosphere above the riometer. But, both the northern and southern beam absorption levels indicate that there is still significant rigidity cutoff influence at this time. The second anomalous period occurs at 14 UT on 9 Nov in the southern (poleward) beam. The theoretical absorption levels increase from ~2 dB to ~4 dB in response to a small increase in K_p from <2 to 3^+. This is not seen in the observed absorption.

Figures 3, 4, and 5 show plots in the same format as Figure 2, and represent SPEs occurring during 26-29 November 2000, 5-8 November 2001, and 28-31 October 2003 respectively. The peak proton >10 MeV fluxes were 942, 31700, and 29500 protons cm^{-2} str^{-1} s^{-1} while the maximum K_p values were 6^+, 9^-, and 9 respectively. Thus Figure 3 represents a small SPE, and Figures 4 and 5 represent two very large SPEs, with the latter cases associated with very large geomagnetic disturbances.

Although the proton fluxes are significantly lower during the 26-29 November 2000 SPE when compared with the 8-11 November 2000 event, the maximum K_p values are the same (6^+). Thus these two events are comparable in many ways. Figure 3 shows that the theoretical absorption levels in the southern (poleward) and northern (equatorward) beams are over estimated in comparison with the absorption data, particularly when K_p=~6 in the northern (equatorward) beam, and K_p=4-6 in the southern (poleward) beam. This is particularly apparent when the proton fluxes are high, and the absorption levels significantly elevated. Of the twenty three 3-hourly bins where proton fluxes are high, 9 show significant over estimates (~0.5-1 dB) in the

predicted absorption in the southern (poleward) beam, while only 5 over estimates occur in the northern (equatorward) beam.

The two large storms shown in Figure 4 and 5 have a wider range of K_p values, but follow similar patterns of behavior as Figure 3. The northern (equatorial) beam shows good agreement between the theoretical absorption and the observed data until K_p>~6. Under these conditions the theoretically determined rigidity cutoffs predict very little influence of cutoff rigidity (i.e., low cutoff energies) on the proton fluxes and thus high absorption levels, but the observed absorption levels are more consistent with K_p=~5 and thus a significant influence due to rigidity cutoffs limiting the proton fluxes. The southern (poleward) beam shows good agreement between theoretical absorption levels and observed absorption for very high K_p (K_p>6), but over estimated absorptions when K_p=4-6. During high K_p (K_p>6) the theory predicts, and the observations show, that there is little or no cutoff rigidity affect on the absorption levels for this beam location. Of the twenty three 3-hourly bins where proton fluxes are high in Figure 4, six show significant over estimates (~2 dB) in the predicted absorption in the southern (poleward) beam, while only 3 over estimates occur in the northern (equatorward) beam. Of the nineteen 3-hourly bins where proton fluxes are high in Figure 5, five show significant over estimates (~2 dB) in the predicted absorption in the southern (poleward) beam, while 8 over estimates occur in the northern (equatorward) beam. This represents an unusual event because the northern beam is less well modeled than the southern beam. The primary reason is because of the unusually long-lasting very high K_p levels leading to less errors in the southern beam in comparison with the northern beam.

The Halley riometer data during the SPE of 5-8 November 2001 was previously used to test the improved rigidity cutoff calculations developed by *Rodger et al.* [2006]. The cutoff rigidities were applied to the proton fluxes in the same way as this study, but the SIC model was used to calculate the riometer absorption instead of using the empirical relationship as we do here.

Comparing Figure 4 in this study with Figure 7 of *Rodger et al.* [2006] shows that combining the empirical relationship with rigidity modified proton fluxes agrees closely with the SIC model results. In addition, the right panel of Figure 3 of *Rodger et al.* [2006] showed that the absorptions calculated by the SIC model in the absence of rigidity cutoff effects reproduces the empirical relationship reported by *Kavanagh et al.* [2004].

So far we have described riometer absorption observed during four SPEs that occurred during the southern hemisphere summer, and thus under daytime conditions. In the next section we determine a nighttime relationship between proton fluxes and riometer absorption in order to investigate rigidity cutoff effects during polar winter nighttime conditions.

5. Nighttime riometer absorption using the Sodankylä Ion and Neutral Chemistry Model

As in *Rodger et al.* [2006] we use the SIC model to produce lower ionospheric electron density profiles during SPEs, but this time in the winter-time (i.e. nighttime) *D*-region above the Halley Bay IRIS instrument. During the daytime it is possible to calculate the non-cutoff riometer absorption using >10 MeV proton fluxes through the empirical relationship of *Kavanagh et al.* [2004], confirmed using the SIC model by *Rodger et al.* [2006]. Here we want to investigate the relationship between proton fluxes and riometer absorption during nighttime conditions in order to investigate rigidity cutoff effects during polar winter conditions.

We assume that the proton spectra at the top of the atmosphere will be determined only by the fluxes of experimentally observed proton flux spectra reported by GOES-borne instruments at geosynchronous altitude. The angular distribution of the protons is assumed to be isotropic over the upper atmosphere, which is valid close to the Earth [*Hargreaves*, 1992]. A SIC modeling run has also been undertaken without any proton forcing (i.e., zero proton fluxes), reasonable at Halley for low K_p conditions. The results of the no-forcing "control" SIC-run allow the calculation of "quiet-time" conditions.

Each run of the SIC model is based on a neutral background atmosphere given by MSISE-90 and provides concentration profiles of neutral and ionic species. Following *Banks and Kockarts* [1973; Part A, p. 194], we calculate the electron collision frequencies of N_2, O_2, and He from MSIS and of O and H from SIC using the neutral temperature profile of MSIS, which we can assume to be equal to electron temperature below 100 km. Electron density is obtained from SIC by subtracting the sum of negative ion concentrations from the sum of positive ion concentrations. Finally, we use the method of *Sen and Wyller* [1960] to compute differential absorption dL/dh and integrate with respect to height. This method takes the operational frequency of the riometer into account and assumes a dipole approximation for the geomagnetic field to obtain the electron gyrofrequency at the respective altitude and latitude.

The Sodankylä Ion and Neutral Chemistry (SIC) model is a 1-D chemical model designed for ionospheric D-region studies, solving the concentrations of 65 ions, including 29 negative ions, and 15 neutral species at altitudes across 20–150 km. This study makes use of SIC version 6.9.0. The model has recently been discussed by *Verronen et al.* [2005], building on original work by *Turunen et al.* [1996] and *Verronen et al.* [2002]. A detailed overview of the model was given in *Verronen et al.* [2005]. We summarize here to provide background for this study.

In the SIC model several hundred reactions are implemented, plus additional external forcing due to solar radiation (1–422.5 nm), electron and proton precipitation, and galactic cosmic radiation. Initial descriptions of the model are provided by *Turunen et al.* [1996], with neutral species modifications described by *Verronen et al.* [2002]. Solar flux is calculated with the SOLAR2000 model (version 2.27) [*Tobiska et al.*, 2000]. The scattered component of solar Lyman-α flux is included using the empirical approximation given by *Thomas and Bowman* [1986]. The SIC code includes vertical transport [*Chabrillat et al.*, 2002] which takes into account molecular [*Banks and Kockarts*, 1973] and eddy diffusion with a fixed eddy diffusion coefficient profile. The background neutral atmosphere is calculated using the MSISE-90 model

275 [*Hedin*, 1991] and tables given by *Shimazaki* [1984]. Transport and chemistry are advanced in
276 intervals of 5 or 15 minutes. While within each interval exponentially increasing time steps are
277 used because of the wide range of chemical time constants of the modeled species.

278 Daytime absorption has been shown to be described by proton fluxes with energies >10 MeV.
279 However, during nighttime conditions the undisturbed D-region has lower electron number
280 densities, such that lower energy protons are expected to play a significant role. Nighttime
281 ionization conditions are more complicated than during the day, with a negative charge transition
282 from electrons to negative ions occurring at sunset [*Verronen et al.*, *2006*] as a result of changes
283 in atomic oxygen. Thus we would expect different relationships between absorption and solar
284 proton fluxes at night than during the day. Figure 6 shows the relationship found between SIC
285 calculated polar nighttime riometer absorption and proton fluxes with energies >5 MeV, taken
286 from the proton fluxes which occurred during the January 2005 SPE. These calculations indicate
287 that nighttime absorption is proportional to (>5 MeV proton flux)$^{0.75}$. This finding differs from
288 the daytime relationship, not only in the power, but also the proton flux threshold. This agrees
289 with previous work on nighttime absorption calculations, which suggested a threshold of 1-5
290 MeV [*Sellers et al., 1977*], although both day and night calculations in that study used a square
291 root power relationship. A lower threshold of >5 MeV during nighttime means that K_p would
292 have to be lower in order to cutoff the same fraction of the proton fluxes as during the day. The
293 lower energy threshold is also consistent with the riometer absorption coming from higher
294 altitudes during the night than the day.

295 During the period when IRIS data from Halley is available there was one significant SPE in
296 nighttime conditions. In Figure 7 we show the observed and calculated absorption during the
297 large SPE of 13-16 July 2000. The format of the plot is the same as Figures 2-5. To calculate the
298 theoretical absorption values we have used the relation Absorption = 0.001×(>5 MeV proton
299 flux)$^{0.75}$. The plot shows that the theoretical and observed absorption values agree well, with

300 overestimates in the theoretically predicted absorptions occurring only on the southern
301 (poleward) beam when K_p>7. No significant periods of over estimation occur on the northern
302 (equatorward) beam. Of the eleven 3-hourly bins where proton fluxes are high in Figure 7, five
303 show significant over estimates (~0.5 dB) in the predicted absorption in the southern (poleward)
304 beam, while four over estimates occur in the northern (equatorward) beam.

305 Notably there are almost no data points in Figure 7 where either the predicted absorption or the
306 observed absorption reach the same levels as the non-cutoff values during high proton fluxes
307 (mainly 15 July). This is despite very high K_p values, and is partly as a result of the rigidity
308 model limiting K_p to a maximum of 6, and also a result of the >5 MeV energy threshold used
309 during the night. At the latitude of Halley IRIS northern (equatorward) beam the proton cutoff
310 energy limit for K_p=6 is ~9 MeV [*Rodger et al.*, 2006]. This means that protons with energies
311 >9 MeV will reach to the latitude of this beam, but energies less than that will not be able to
312 make it so far equatorward. During the day, when a >10 MeV proton flux energy threshold for
313 the absorption calculation applies, and the K_p-dependent rigidity cutoff is ~9 MeV, 100% of the
314 >10 MeV GOES proton fluxes will penetrate to that location, and thus contribute to the riometer
315 absorption. However, during the night when a >5 MeV proton flux energy threshold applies, and
316 the K_p-dependent rigidity cutoff is ~9 MeV, the calculations predict that only ~30-90% of the
317 >5 MeV GOES proton fluxes penetrate to that location and contribute to the riometer absorption.
318 Note that the 30-90% range is determined by the proton spectra, i.e., what percentage of the total
319 proton number flux is greater than the rigidity cutoff energy. Thus at nighttime the only time that
320 the predicted absorption gets close to the non-rigidity cutoff levels is on those occasions when
321 the proton spectrum is very hard, i.e., there are high fluxes of protons with high energy
322 (>10 MeV) in comparison with the lower energy protons (5-10 MeV).

323

324 7. Discussion

325 We have investigated the rigidity cutoff model developed by *Rodger et al.* [2006] based on
326 previous work by *Smart and Shea* [2003]. Using a study of riometer absorption data during four
327 daytime SPEs, i.e., high latitude summer measurements where the Sun is above the horizon all
328 the time, we have shown that it is possible to reproduce the riometer data using a simple
329 empirical relationship based on the incident proton fluxes, and a K_p-limited rigidity calculation.
330 For the southern (poleward) beam of the Halley IRIS K_p=6 represents a rigidity cutoff energy of
331 0.0 MeV, and once K_p=6 is reached the predicted absorption is the same as the non-rigidity
332 absorption levels. This can be seen in Figure 3 at the beginning of 27 Nov 2000, where the
333 asterisks (rigidity calculation) overlap the short dashed line values (non-rigidity calculation).
334 However, the observed absorption is not consistent with this picture, and when K_p>4 the
335 predicted absorption is also over estimated. This suggests that the rigidity cutoff limit (K_p=6,
336 0.0 MeV for the southern beam) needs to be higher than the proton flux energy threshold
337 (10 MeV in daytime). Either decreasing the K_p "saturation" limit, or lowering the proton flux
338 energy threshold can achieve this.
339 During the two large SPEs, when K_p approached 9, the southern (poleward) beam absorption
340 was close to that of the calculated rigidity and non-rigidity cutoff absorption levels (Figures 4
341 and 5), whereas this was not true when K_p=4-6 in the previous analysis. This clearly indicates
342 that the K_p=6 saturation limit to the rigidity cutoff model is too low and needs to be higher.
343 For the northern (equatorward) beam of the Halley IRIS K_p=6 represents a rigidity cutoff
344 energy of 9 MeV, thus the rigidity cutoff energy and the proton flux energy threshold (10 MeV)
345 are similar, and when K_p=6 is reached the predicted absorption values are the same as the non-
346 rigidity levels. However, the observed absorption does not reach the non-rigidity level during
347 high proton fluxes, and as a result this suggests that the K_p=6 saturation limit is too high or the
348 absorption threshold is too high.

Absorption data from the single nighttime SPE (July 2000) is reasonably modeled using a >5 MeV proton flux energy threshold. The behavior of the observed absorption on the southern (poleward) beam is very similar to the daytime examples in that the predicted absorption is over estimated when $K_p \geq 6$. This is because at $K_p=6$ the rigidity cutoff energy is 0.0 MeV which is lower than the proton flux energy threshold of >5 MeV. The northern (equatorward) beam behavior is slightly different from the daytime case because for $K_p=6$ the rigidity cutoff energy (9 MeV) is more than the proton flux energy threshold (>5 MeV), and thus although the predicted absorption is still an overestimate at high K_p, it is not as large as the maximum non-cutoff case.

Using the rigidity cutoff model of *Rodger et al.* [2006] and empirical estimates of riometer absorption from proton fluxes we have been able to reproduce the absorption seen by the Halley riometer at two *L*-shells (L=4.32 and 4.80). Typically reasonable estimates of absorption were made 58-74 % of the time for the southern (poleward) beam, and 65-87 % of the time for the northern (equatorward) beam. The success of the *Rodger et al.* [2006] rigidity cutoff model is dependent on a balance between the rigidity cutoff energy for the protons at any given *L*-shell, and the proton flux energy threshold for the protons. At the times when the empirical estimates are in error there is usually an over estimate in the predicted absorption levels, caused by the $K_p=6$ saturation limit used in the rigidity cutoff calculation. In order to improve the success rate for the northern (equatorward) beam the K_p saturation limit in the rigidity model would have to be decreased to $K_p=5.5$ or the daytime proton flux energy threshold decreased to >5 MeV. For the southern beam changing the K_p saturation limit to 5 would be more appropriate, but no changes of the daytime proton flux energy threshold would make any significant effect.

Changing the proton flux energy threshold introduces significant difficulties in modeling the riometer absorption because of hysteresis in the relationship between the proton fluxes and absorption for any proton flux energy threshold values other than 10 MeV during the day and

374 5 MeV during the night. Thus we restrict ourselves here to investigate the effects of the K_p
375 saturation limit used in the rigidity cutoff calculation. Figure 8 shows the northern and southern
376 beam absorption during the solar proton event of 05-08 November 2001. The figure is the same
377 format as Figure 4, except that the saturation limit has been changed to K_p=5, and the location of
378 the southern (poleward) beam moved by 0.6° equatorwards. These changes have the effect of
379 increasing the rigidity cutoff energy for the northern beam from 9 MeV to 28 MeV, and
380 increasing the rigidity cutoff energy for the southern beam from 0.0 MeV to 8 MeV. In practice
381 this means that the northern beam does not achieve the non-rigidity cutoff absorption maximum
382 during this storm, in agreement with the observations. Generally the Halley northern
383 (equatorward) beam will not achieve the non-rigidity cutoff absorption maximum unless the
384 proton spectrum is very hard and has little flux between 10-28 MeV. The southern beam will still
385 experience absorption at the non-cutoff maximum, but the more equatorward location of the
386 beam results in lower levels of absorption when K_p is just below the saturation limit. Both of
387 these effects result in much better agreement between the calculated absorption and the observed
388 absorption for this large geomagnetic storm in comparison with the results shown in Figure 4.
389 However, for moderately disturbed solar proton events, where K_p remains close to the
390 saturation limit the calculated absorption is not in such good agreement with the observations.
391 Figure 9 shows the adjusted absorption for the 26-29 November 2000 period to be contracted
392 with Figure 3. The K_p=5 saturation limit has reduced the northern beam absorption, and reduced
393 the southern beam absorption when K_p is close to the K_p=5 saturation limit. However, during
394 higher K_p the southern beam does not experience the maximum non-rigidity cutoff absorption
395 levels that the relocated beam calculations predict. Overall there is a 50% decrease in the number
396 of 3-hour data bins that previously showed poor agreement between the calculated and observed
397 absorption.

The adjustments to the rigidity cutoff calculations made here are relatively subtle. By changing the location of the southern (poleward) beam better agreement between theory and observations is obtained at times, and this indicates that initially the two beam locations were too far apart (i.e., smaller than the 2° of latitude assumed initially). The adjusted location for the southern (poleward) beam represents a separation from the northern beam of 1.4° of latitude, which can be interpreted as indicating that the dominant altitude that the absorption is occurring at lower altitude i.e., 60 km instead of the 90 km initially assumed. The lower K_p saturation limit improves the agreement between theory and observations, particularly on the northern (equatorward) beam during most geomagnetic conditions. The K_p change has little effect on the southern (equatorward) beam, which appears more sensitive to changes in beam location. This suggests that at L>4.5, and for high K_p, significant changes in L-shell location have occurred for the beam, in particular that the geographic location of the beam has moved to a lower L-shell. Some of this change can be accommodated by the lowering of the peak absorption altitude of the southern beam, which equates to a shift equatorwards for this riometer beam as K_p increases and greater latitudinal penetration of proton fluxes occur.

For large geomagnetic storms, such as that of 05-08 November 2001, the adjustments made here to the *Rodger et al.* [2006] rigidity cutoff model allow us to improve the absorption estimates. In Figure 10 we plot the predicted southern hemisphere absorption levels during the high proton flux period that occurred at 00 UT on 06 Nov 2001, when K_p reached 8^+. This calculation was undertaken using the improved rigidity cutoff model. The plot shows the region of high absorption with levels of 14 dB, where all protons with energies greater than 10 MeV can access the polar atmosphere (i.e., rigidity cutoff effects are unimportant to the riometer absorptions). Surrounding this contour is an outer region where the absorption levels gradually reduce to the limits of detectability for most riometers (roughly 0.1 dB). This can be thought of

422 as an extreme example of SPE-produced riometer absorptions, occurring when both K_p and
423 proton fluxes are very high. The outer zone of rigidity influenced absorption lies mostly at 50°S,
424 except in the region of the Antarctic Peninsula where it is located at ~70°S. From the riometer
425 absorption calculations we can see that the transition in access levels for energetic protons to the
426 stratosphere and mesosphere is controlled by geomagnetic rigidity, with the shift from no-access
427 to total access occurs over the range L=3-4.5, or across ~10° of latitude. For locations which are
428 equatorward of the limits of the outer zone shown in Figure 10, SPEs should never lead to
429 significant changes in riometer data. This provides an indication as to the limits inside which
430 SPEs can play a role in modifying the neutral chemistry of the stratosphere and mesosphere
431 [Verronen, 2005].
432
433 **8. Summary**
434 In the polar atmosphere, significant chemical and ionization changes occur during solar proton
435 events. The access of solar protons to this region is limited by the dynamically changing
436 geomagnetic field. In this study we have used riometer absorption observations to investigate the
437 accuracy of a model to predict K_p-dependent geomagnetic rigidity cutoffs, and hence the
438 changing proton fluxes. The imaging riometer at Halley, Antarctica is ideally situated for such a
439 study, as the rigidity cutoff sweeps back and forth across the instrument's field of view,
440 providing a severe test of the rigidity cutoff model. Specifically we investigate the accuracy of
441 the rigidity cutoff model developed by Smart and Shea [2003], and improved by Rodger et al.
442 [2006]. Using observations from the Halley riometer during five solar proton events, we have
443 confirmed the basic accuracy of this rigidity model. However, we have shown that although the
444 rigidity cutoff model can be used to reasonably estimate the absorption due to precipitating
445 proton fluxes, it can be further improved by setting a lower K_p limit (i.e. K_p=5 instead of 6) at

446 which the rigidity process saturates. We also find that for L>4.5 there is significant change in the
447 geomagnetic location of a riometer beam during a large geomagnetic storm, such that the
448 apparent L-shell of the beam moves equatorward. This is in part explained by the decreasing
449 altitude of peak riometer absorption as protons penetrate more readily at higher K_p into the
450 rigidity dominated zone.

451 We have also used the Sodankyla Ion and Neutral Chemistry model to determine an empirical
452 relationship between integral proton precipitation fluxes and nighttime ionosphere riometer
453 absorption, in order to allow consideration of winter time SPEs. We find that during the
454 nighttime the proton flux energy threshold is lowered to protons with energies of >5 MeV in
455 comparison with >10 MeV during the daytime.

456 Where both K_p and proton fluxes are very high the transition in access levels for energetic
457 protons to the stratosphere and mesosphere is controlled by geomagnetic rigidity, with the shift
458 from no-access to total access occurs over the range L=3-4.5, or across ~10° of latitude. The
459 outer zone of rigidity influenced absorption lies mostly at 50°S, except in the region of the
460 Antarctic Peninsula where it is located at ~70°S. In the northern hemisphere this will equate to
461 ~45°N. These latitude bounds provide an indication as to the limits inside which SPEs can play a
462 role in modifying the neutral chemistry of the stratosphere and mesosphere.

463

464 **Acknowledgments.** CJR and MAC would like to thank Lauren Farnden of Dunedin for her
465 support. This research was supported by the New Zealand International Science and Technology
466 (ISAT) Linkages Fund. The Halley IRIS system was funded in part by a grant from the National
467 Science Foundation to the University of Maryland, and by the Natural Environment Research
468 Council (NERC).

469

469 **References**

470 Banks, P. M., and G. Kockarts, *Aeronomy*, vol. B, chap. 15, Academic Press, 1973.

471 Birch, M. J., J. K. Hargreaves, A. Senior, and B. J. I. Bromage (2005), Variations in cutoff
472 latitude during selected solar energetic proton events, *J. Geophys. Res.*, 110, A07221,
473 doi:10.1029/2004JA010833.

474 Boberg, P. R. Jr., E. O. Flückiger, and E. Kobel, Geomagnetic transmission of solar energetic
475 protons during the geomagnetic disturbances of October 1989, *Geophys. Res. Lett.,* 22(9),
476 1133-1136, 10.1029/95GL00948, 1995.

477 Chabrillat, S., G. Kockarts, D. Fonteyn, and G. Brasseur, Impact of molecular diffusion on the
478 CO_2 distribution and the temperature in the mesosphere, *Geophys. Res. Lett.*, 29, 1-4, 2002.

479 Hargreaves, J. K., *The solar-terrestrial environment*, Atmospheric and Space Science Series,
480 Cambridge University Press, Cambridge, UK, 1992.

481 Hargreaves, J. K., and M. J. Jarvis, The multiple riometer system at Halley, Antarctica, *British*
482 *Antarctic Surv. Bull.*, 72, 13-23, 1986.

483 Hedin, A. E., Extension of the MSIS Thermospheric model into the middle and lower
484 Atmosphere, *J. Geophys. Res.*, 96, 1159-1172, 1991.

485 Kavanagh, A. J., S. R. Marple, F. Honary, I. W. McCrea, and A. Senior , On solar protons and
486 polar cap absorption: constraints on an empirical relationship, *Ann. Geophys.*, 22(4), 1133-
487 1147, 2004.

488 Kress B. T., M. K. Hudson, K. L. Perry, and P. L. Slocum, Dynamic modeling of geomagnetic
489 cutoff for the 23–24 November 2001 solar energetic particle event, *Geophys. Res. Lett.*, 31,
490 L04808, doi:10.1029/2003GL018599, 2004.

491 Krishnaswamy, S., D. L. Detrick, and T. J. Rosenberg, The inflection point method of
492 determining riometer quiet day curves, *Radio Sci.*, 20, 123-136, 1985.

493 Little, C. G, and H. Leinbach, The riometer - a device for the continuous measurement of
494 ionospheric absorption, *Proceedings of the IRE*, 47, 315-319, 1959.
495 Ogliore, R. C., R. A. Mewaldt, R. A. Leske, E. C. Stone, and T. T. von Rosenvinge, A direct
496 measurement of the geomagnetic cutoff for cosmic rays at space station latitudes, *Proceedings*
497 *of ICRC 2001*, 4112-4115, Copernicus Gesellschaft, 2001.
498 Rodger, C. J., M. A. Clilverd, P. T. Verronen, Th. Ulich, M. J. Jarvis, and E. Turunen, Dynamic
499 geomagnetic rigidity cutoff variations during a solar proton event, J. Geophys. Res., 111,
500 A04222, doi:10.1029/2005JA011395, 2006.
501 Rose, M. C., M. J. Jarvis, M. A. Clilverd, D. J. Maxfield, and T. J. Rosenberg, The effect of
502 snow accumulation on imaging riometer performance, *Radio Sci.*, 35, 1143-1153, 2000.
503 Selesnick, R. S., A. C. Cummings, J. R. Cummings, R. A. Mewaldt, E. C. Stone, and T. T. von
504 Rosenvinge, Geomagnetically trapped anomalous cosmic rays, *J. Geophys. Res.*, 100, 9503-
505 9518, 1995.
506 Sellers, B., F. A. Hanser, M. A. Stroscio, and G. K. Yates (1997), The night and day
507 relationships between polar cap riometer absorption and solar protons, *Radio Sci.,* 12, 779-
508 789.
509 Sen, H. K., and A. A. Wyller, On the generalization of the Appleton-Hartree magnetoionic
510 formulas, *J. Geophys. Res.*, 65, 3931-3950, 1960.
511 Shimazaki, T., *Minor Constituents in the Middle Atmosphere (Developments in Earth and*
512 *Planetary Physics, No 6)*, D. Reidel Publishing Co., Dordrecht, Netherlands, 1984.
513 Shirochkov, A., L. N. Makarova, S. N. Sokolov, and W. R. Sheldon (2004), Ionospheric effects
514 of the simultaneous occurrence of a solar proton event and relativistic electron precipitation as
515 recorded by ground-based instruments at different latitudes, J. Atmos. Sol. Terr. Phys., 66,
516 1035– 1045.

517 Smart, D. F., and M. A. Shea, Geomagnetic cutoffs - a review for space dosimetry applications,
518 *Adv. Space Res.*, 14(10), 787-796, 1994.
519 Smart, D. F., and M. A. Shea, Comparison of the Tsyganenko model predicted and measured
520 geomagnetic cutoff latitudes, *Adv. Space Res.*, 28(12), 1733-1738, 2001.
521 Smart, D. F., and M. A. Shea, The space developed dynamic vertical cutoff and its applicability
522 to aircraft radiation dose, *Adv. Space Res.*, 32(1), 103-108, 2003.
523 Smart, D. F., M. A. Shea, M. J. Golightly, M. Weyland, and A. S. Johnson, Evaluation of the
524 dynamic cutoff rigidity model using dosimetry data from the STS-28 flight, *Adv. Space Res*.,.
525 31(4), 841-846, 2003.
526 Stauning, P., Ionospheric investigations using imaging riometer observations, in *Review of Radio*
527 *Science 1993-1996,* edited by W. R. Stone, pp. 157-161, Oxford Univ. Press, Oxford,
528 England, 1996.
529 Thomas, L., and M. R. Bowman, A study of pre-sunrise changes in negative ions and electrons in
530 the D-region, *J. Atmos. Terr. Phys.*, 4, 219, 1986.
531 Tobiska, W. K., T. Woods, F. Eparvier, R. Viereck, L. D. B. Floyd, G. Rottman, and O. R.
532 White, The SOLAR2000 empirical solar irradiance model and forecast tool, *J. Atmos. Terr.*
533 *Phys.*, 62, 1233-1250, 2000
534 Tsyganenko, N. A., Determination of magnetospheric current system parameters and
535 development of experimental geomagnetic models based on data from IMP and HEOS
536 satellites, *Planet. Space Sci.*, 37, 5-20, 1989.
537 Turunen, E., H. Matveinen, J. Tolvanen, and H. Ranta, D-region ion chemistry model, in *STEP*
538 *Handbook of Ionospheric Models*, edited by R. W. Schunk, pp. 1-25, SCOSTEP Secretariat,
539 Boulder, Colorado, USA, 1996.

Verronen, P. T., E. Turunen, Th. Ulich, and E. Kyrölä, Modelling the effects of the October 1989 solar proton event on mesospheric odd nitrogen using a detailed ion and neutral chemistry model, *Ann. Geophys.*, 20, 1967-1976, 2002.

Verronen, P. T., A. Seppälä, M. A. Clilverd, C. J. Rodger, E. Kyrölä, C.-F. Enell, Th. Ulich, and E. Turunen, Diurnal variation of ozone depletion during the October-November 2003 solar proton event, *J. Geophys. Res.*, 110(A9), doi:10.1029/2004JA010932, 2005.

Verronen, P. T., Th. Ulich, E. Turunen, and C. J. Rodger (2006), Sunset transition of negative charge in the D-region ionosphere during high-ionization conditions, *Ann. Geophys*., 24, 187-202.

M. A. Clilverd and T. Moffat-Griffin, Physical Sciences Division, British Antarctic Survey, High Cross, Madingley Road, Cambridge CB3 0ET, England, U.K. (e-mail: macl@bas.ac.uk; tmof@bas.ac.uk)

C. J. Rodger, Department of Physics, University of Otago, P.O. Box 56, Dunedin, New Zealand. (email: crodger@physics.otago.ac.nz).

P. T. Verronen, Earth Observation, Finnish Meteorological Institute, P.O. Box 503 (Erik Palménin aukio 1), FIN-00101 Helsinki, Finland. (email: pekka.verronen@fmi.fi).

561 **Figure 1.** Map showing the region in Antarctica in which our study is undertaken. The square
562 marks the location of Halley (75.6ºS, 26.32°W, *L*=4.6), while the open circles show the northern
563 (equatorward) and southern (poleward) IRIS riometer beams used in our study.

564 **Figure 2.** [Upper panel] The variation of the non-cutoff absorption that would be expected if
565 there were no influence of rigidity on the proton fluxes into the atmosphere (short dashed line)
566 during 08-11 November 2000, compared with the observed absorption on the Halley IRIS
567 southernmost beam 1 (*L*=4.80, solid line). [middle panel] The variation of the non-cutoff
568 absorption as in the upper panel (short dashed line), compared with the observed absorption on
569 the northernmost beam 7, (*L*=4.32, long dashed line). The equivalent absorption levels using
570 rigidity affected proton fluxes for each beam location are also shown (asterisk in the south,
571 diamond in the north). [bottom panel] The variation of K_p during the SPE period. The horizontal
572 dotted line represents the K_p saturation limit used in the rigidity model calculations.

573 **Figure 3.** As Figure 2 but for 26-29 November 2000

574 **Figure 4.** As Figure 2 but for 05-08 November 2001

575 **Figure 5.** As Figure 2 but for 28-31 October 2000

576 **Figure 6.** Comparison between the SIC calculated nighttime cosmic noise absorption for the
577 Halley IRIS parameters and >5 MeV proton fluxes (crosses). The grey columns indicate the
578 number of samples in each energy range (as labeled). A linear fit indicates a clear relationship
579 between the riometer absorption and the proton fluxes.

580 **Figure 7.** As Figure 2, but using the nighttime empirical absorption/proton flux relationship for
581 the wintertime SPE, 13-16 July 2000.

582 **Figure 8.** As Figure 2, but using K_p=5 instead of K_p=6 as the cutoff limit for 05-08 November
583 2001, and with the southern (equatorward) beam moved to a lower *L*-shell.

584 **Figure 9.** As Figure 2, but using K_p=5 instead of K_p=6 as the cutoff limit for 26-29 November
585 2000, and with the southern (equatorward) beam moved to a lower *L*-shell.

586 **Figure 10.** Map of the predicted levels of absorption globally for the peak fluxes during 06 Nov
587 2001 based on the improved K_p-dependent geomagnetic rigidity cutoff model.

588

589

589

590

591

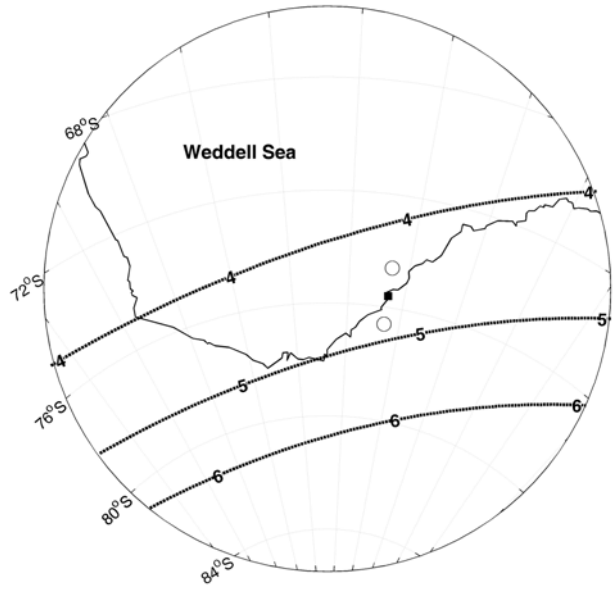

592

593 **Figure 1.** Map showing the region in Antarctica in which our study is undertaken. The square

594 marks the location of Halley (75.6ºS, 26.32°W, *L*=4.6), while the open circles show the northern

595 (equatorward) and southern (poleward) IRIS riometer beams used in our study.

596

597

597

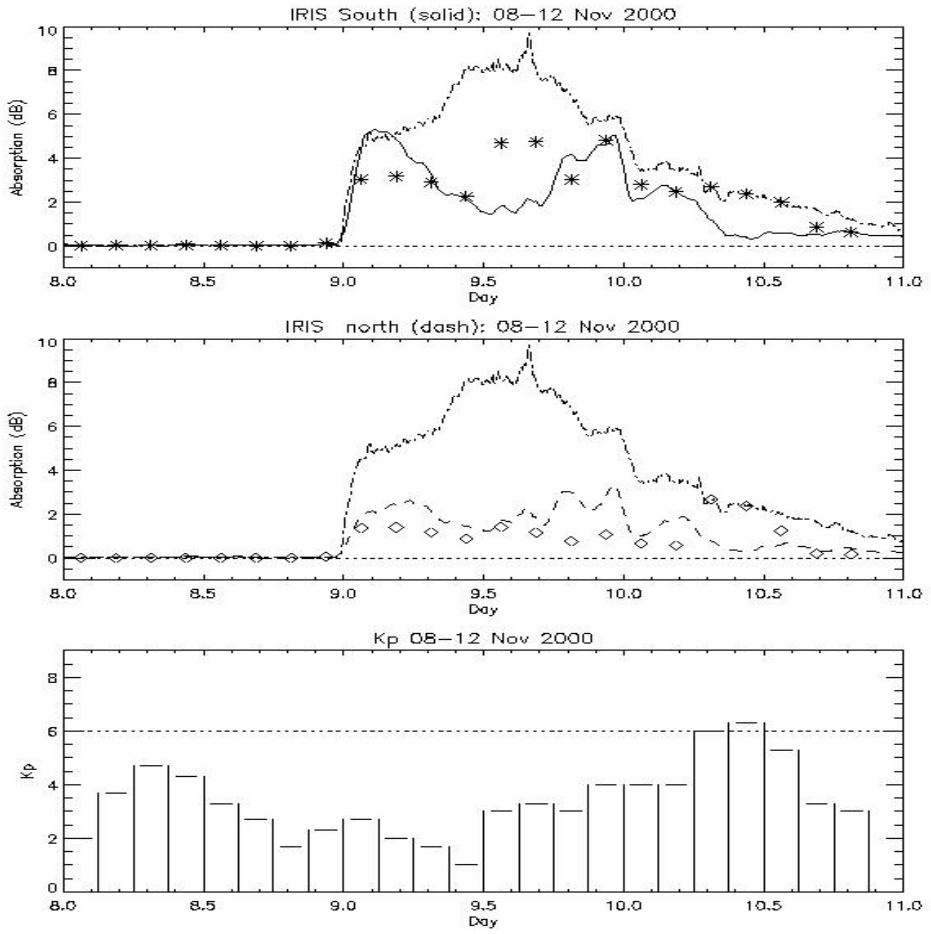

598

599 **Figure 2.** [Upper panel] The variation of the non-cutoff absorption that would be expected if
600 there were no influence of rigidity on the proton fluxes into the atmosphere (short dashed line)
601 during 08-11 November 2000, compared with the observed absorption on the Halley IRIS
602 southernmost beam 1 (L=4.80, solid line). [middle panel] The variation of the non-cutoff
603 absorption as in the upper panel (short dashed line), compared with the observed absorption on
604 the northernmost beam 7, (L=4.32, long dashed line). The equivalent absorption levels using
605 rigidity affected proton fluxes for each beam location are also shown (asterisk in the south,
606 diamond in the north). [bottom panel] The variation of K_p during the SPE period. The horizontal
607 dotted line represents the K_p saturation limit used in the rigidity model calculations.

608

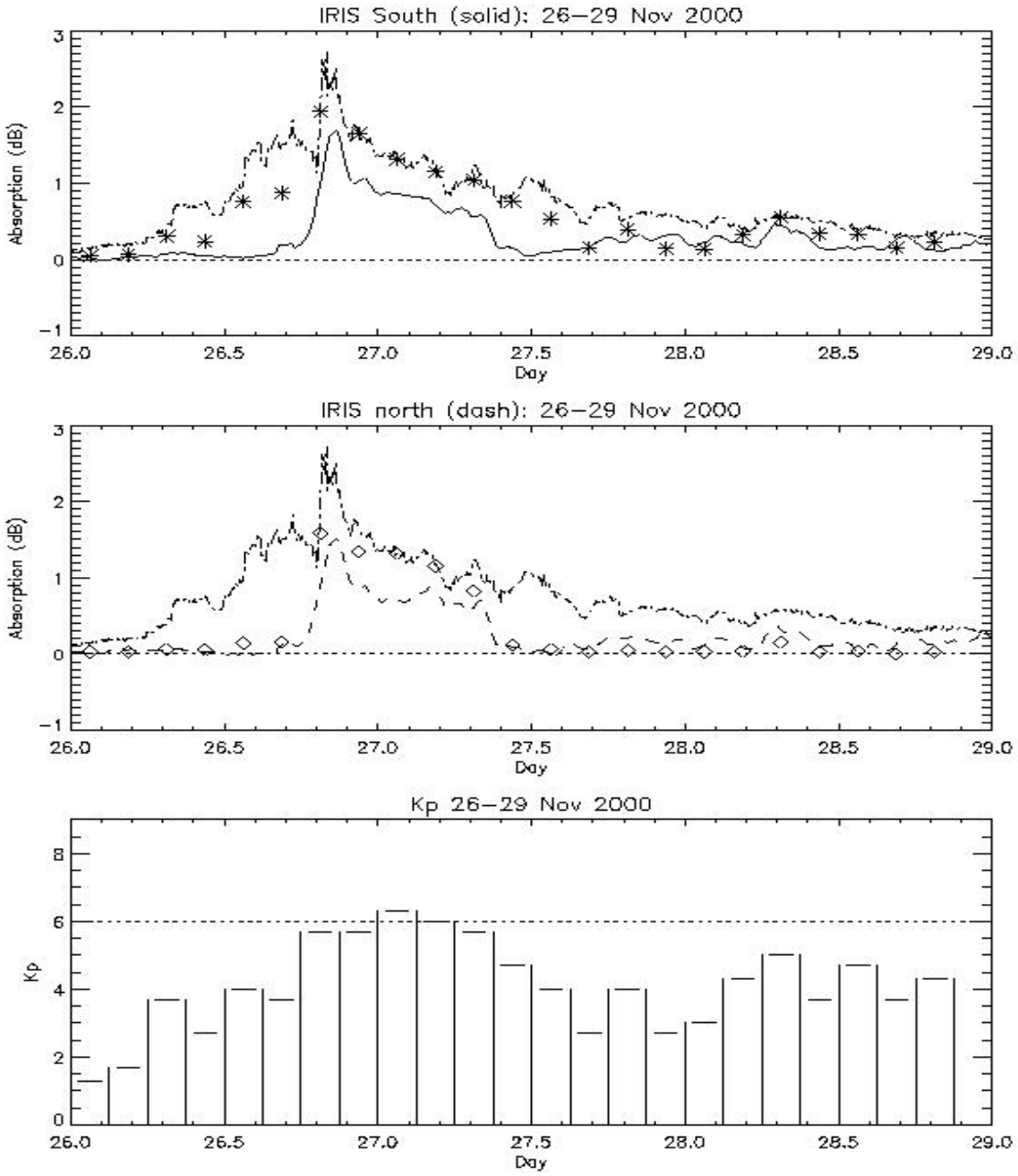

609

610 **Figure 3.** As Figure 2 but for 26-29 November 2000.

611

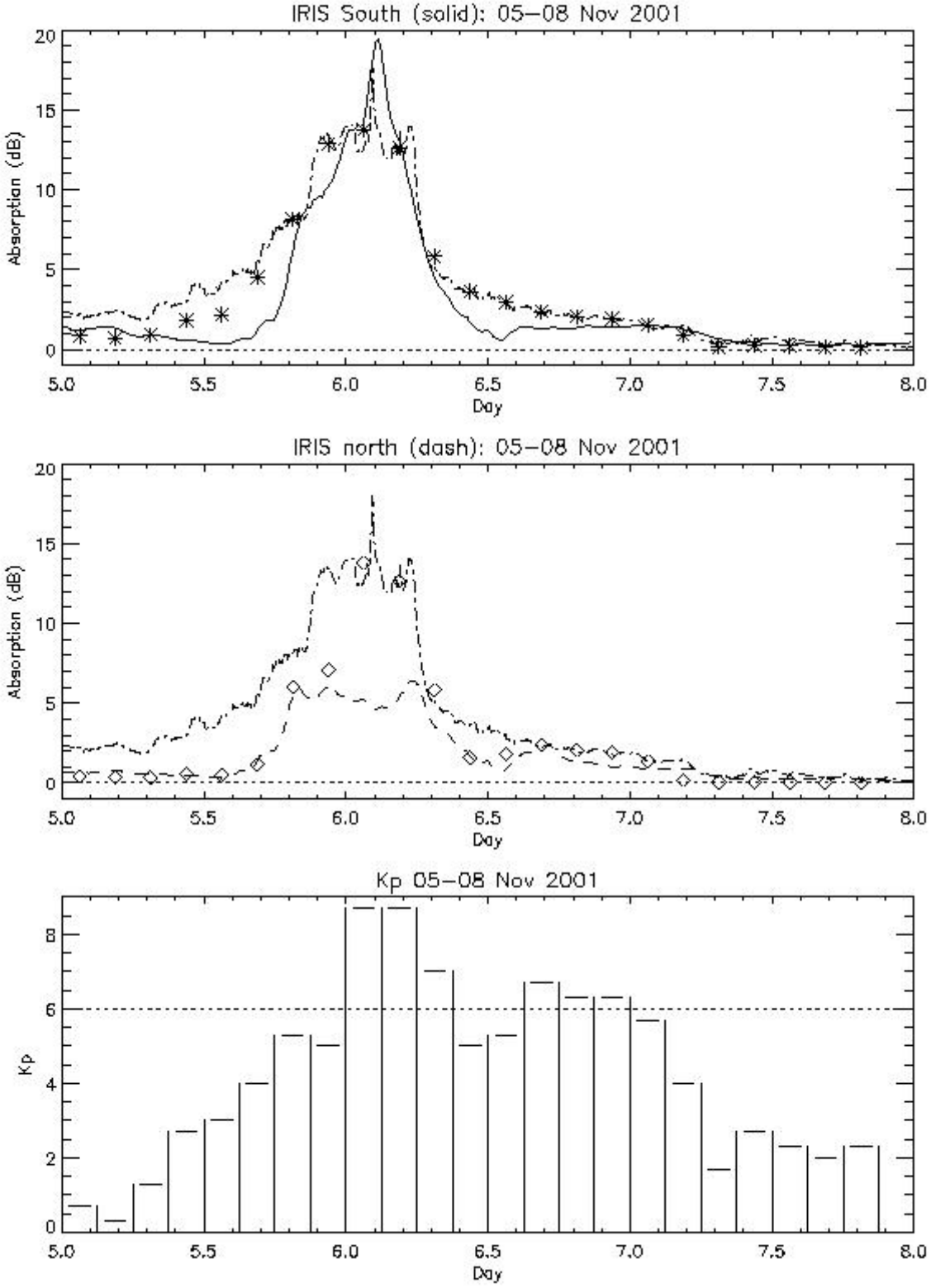

611
612

613 **Figure 4.** As Figure 2 but for 05-08 November 2001

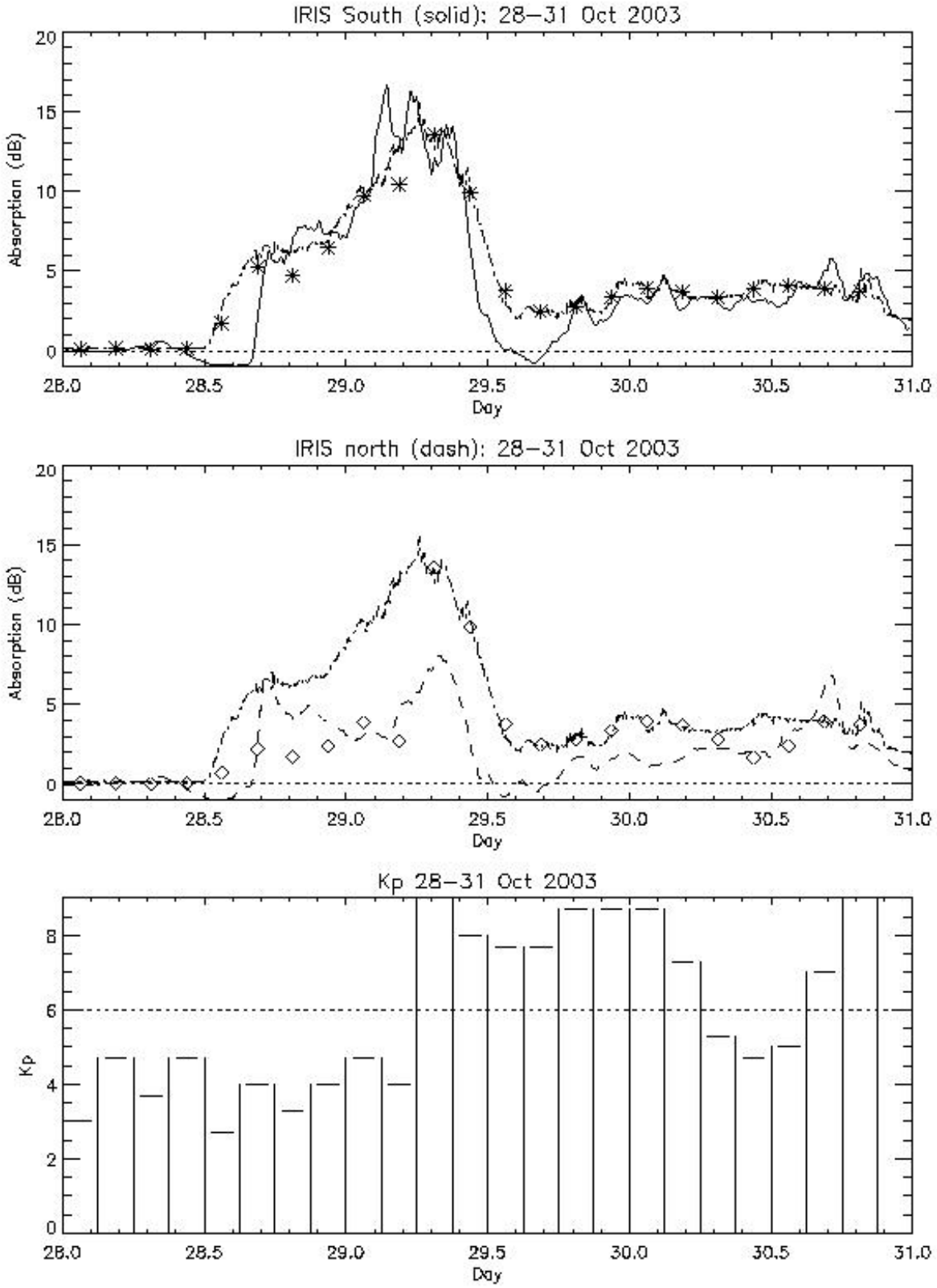

614

615 **Figure 5.** As Figure 2 but for 28-31 October 2003.

616

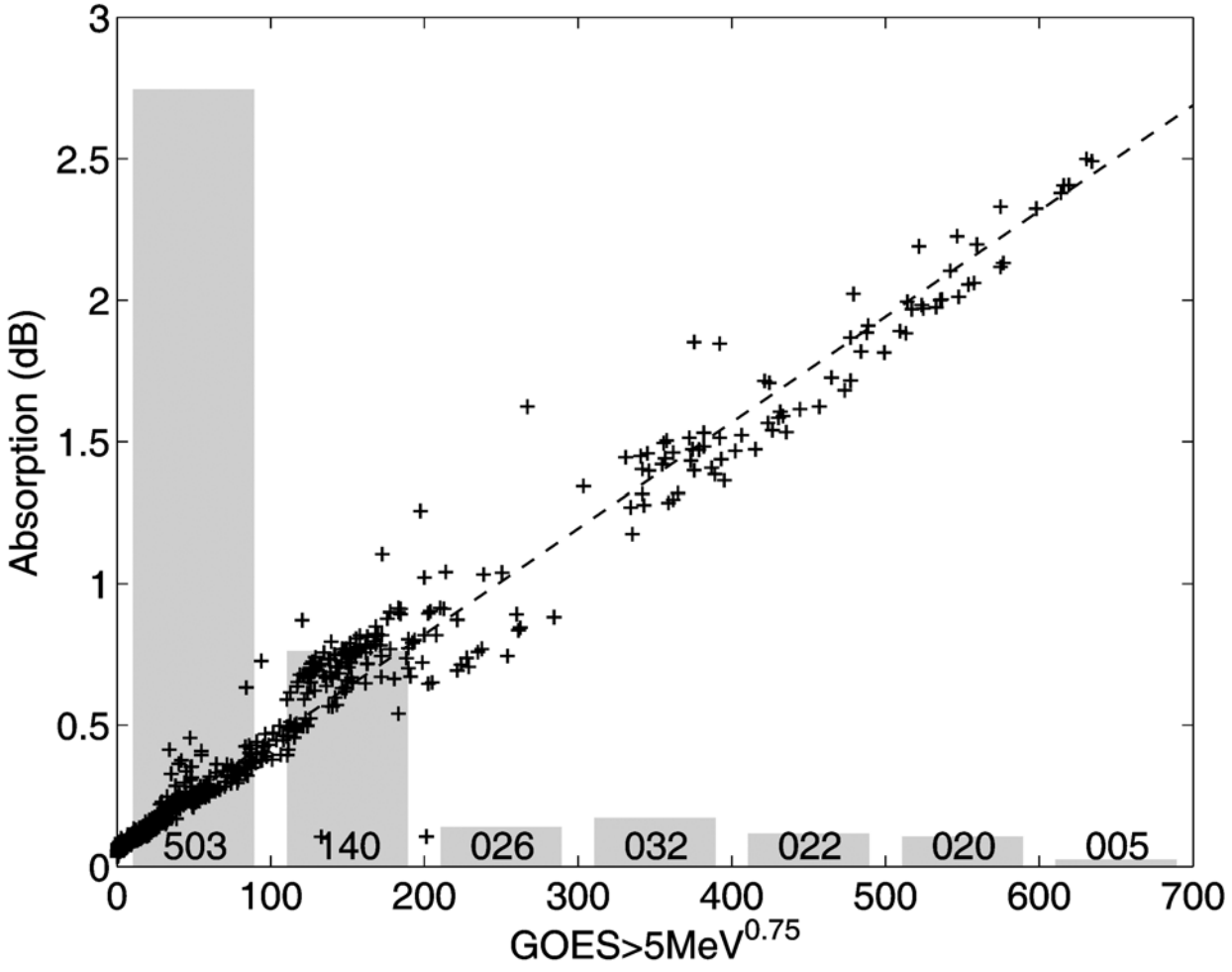

Figure 6. Comparison between the SIC calculated nighttime cosmic noise absorption for the Halley IRIS parameters and >5 MeV proton fluxes (crosses). The grey columns indicate the number of samples in each energy range (as labeled). A linear fit indicates a clear relationship between the riometer absorption and the proton fluxes.

623

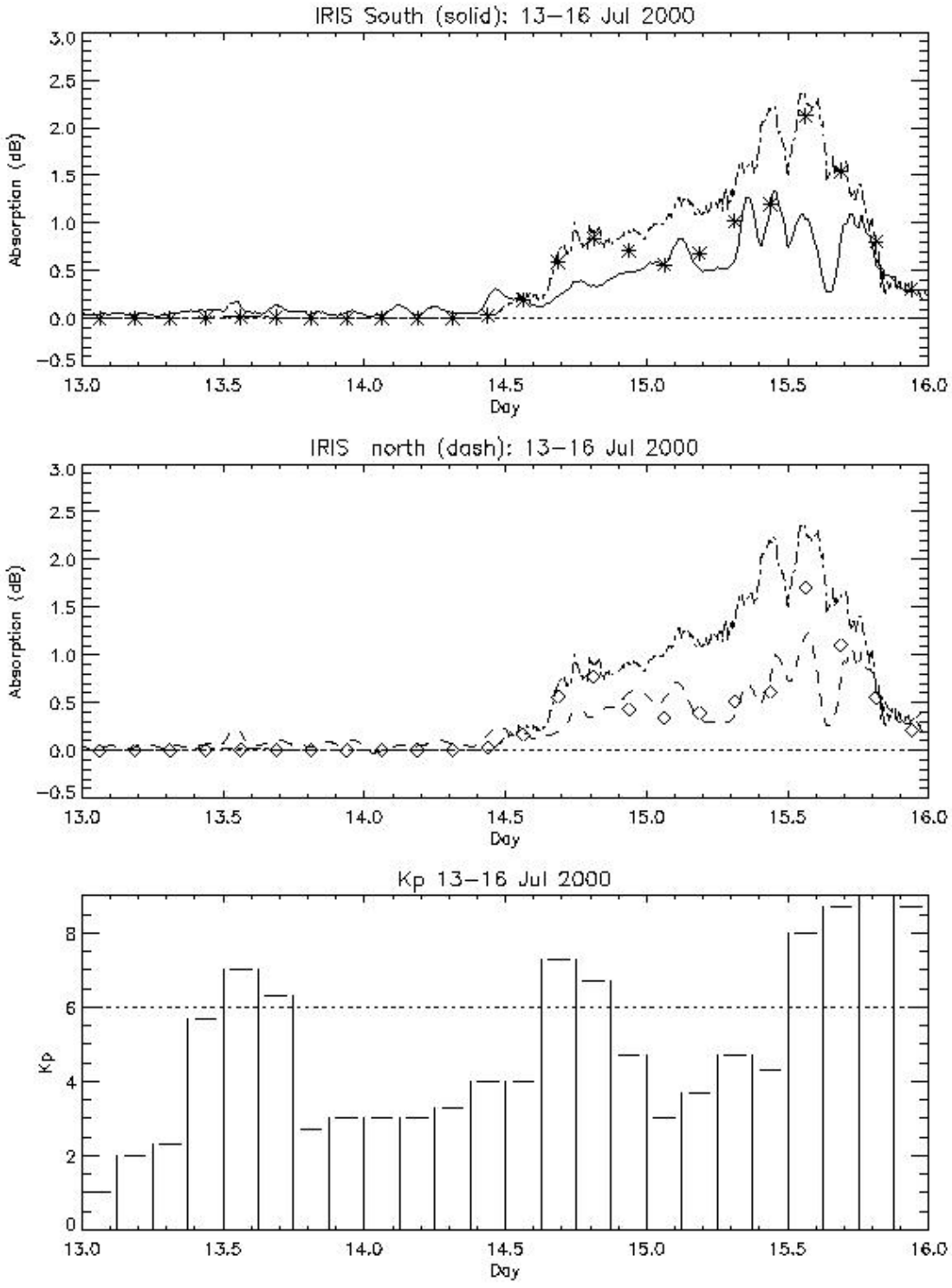

624

625 **Figure 7.** As Figure 2, but using the nighttime empirical absorption/proton flux relationship for

626 the wintertime SPE, 13-16 July 2000.

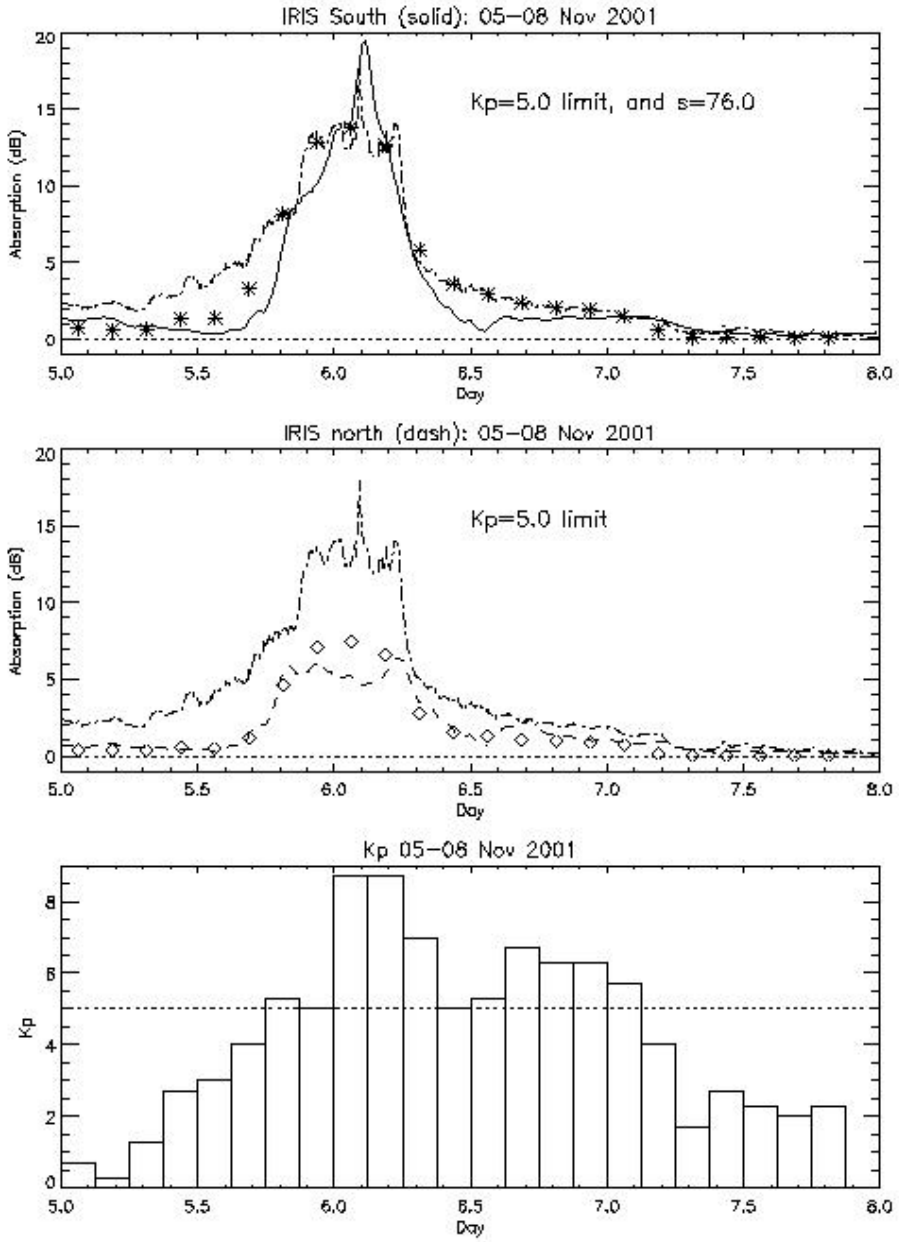

627

628 **Figure 8.** As Figure 2, but using K_p=5 instead of K_p=6 as the cutoff limit for 05-08 November

629 2001, and with the southern (equatorward) beam moved to a lower *L*-shell.

630

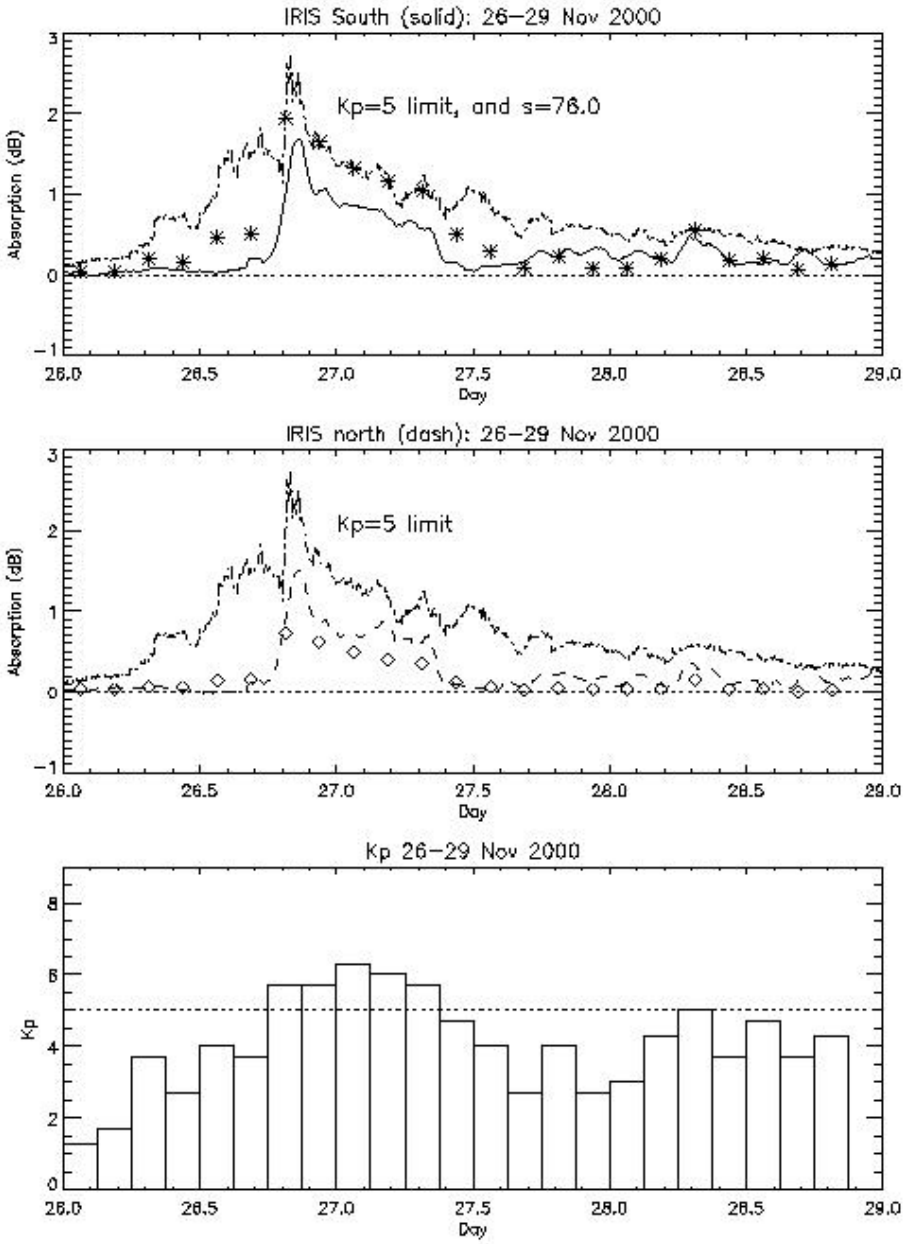

630

631 **Figure 9.** As Figure 2, but using K_p=5 instead of K_p=6 as the cutoff limit for 26-29 November

632 2000, and with the southern (equatorward) beam moved to a lower *L*-shell.

633

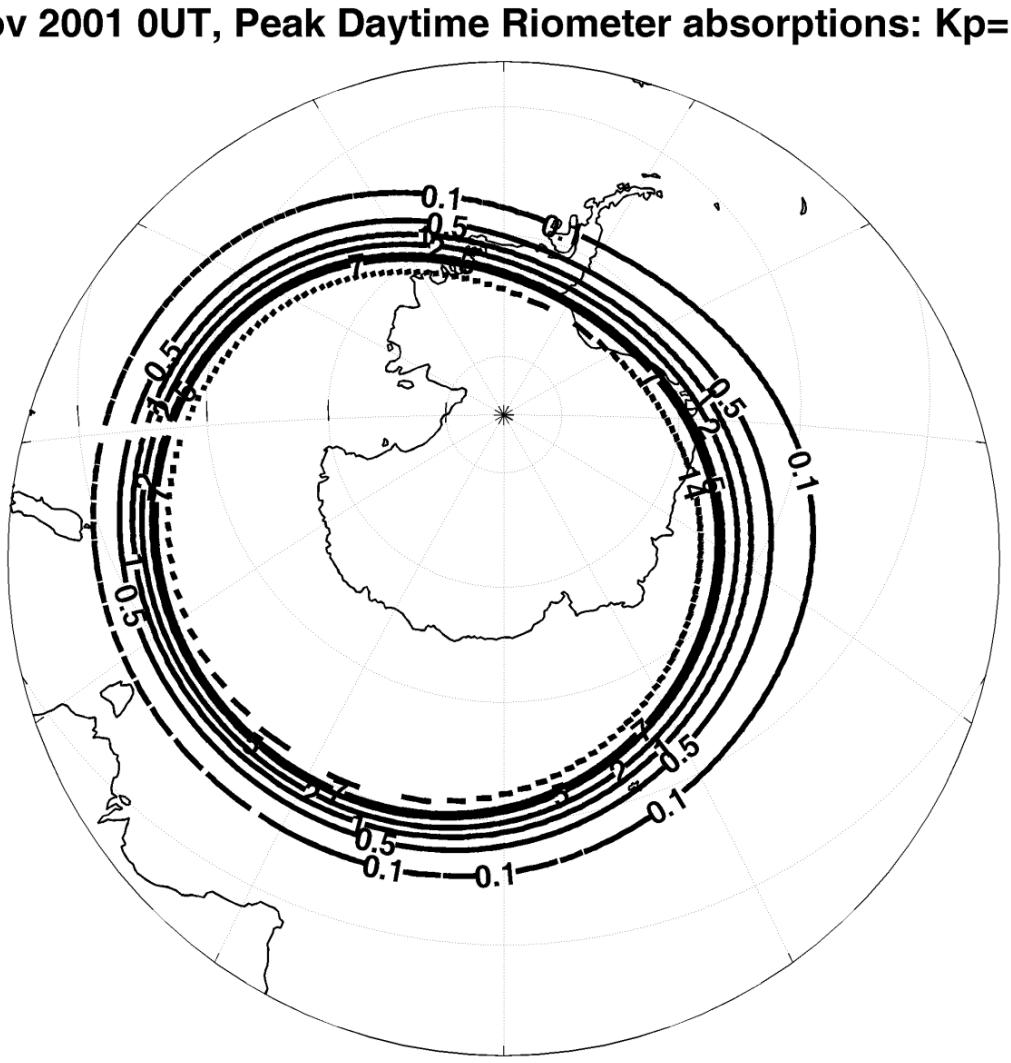

633

634 **Figure 10.** Map of the predicted levels of absorption globally for the peak fluxes during 06 Nov

635 2001 based on the improved K_p-dependent geomagnetic rigidity cutoff model.